Spatially-Resolved Measurement of Dissolved Oxygen in Multi-Stream Microfluidic Devices

Volker Nock, *Member, IEEE,* and Richard J. Blaikie, *Member, IEEE*

***Abstract*— Dissolved oxygen (DO) is an important parameter with significant effect on cellular development and function. Micron-scale laminar flow and hydrodynamic focusing provide ideal tools for the generation of controlled chemical micro-environments and their application as stimuli to cells. In this paper we demonstrate the generation and characterization of multi-stream laminar flow and hydrodynamically focused sample streams with defined dissolved oxygen concentrations on chip. A solid-state oxygen sensor layer was integrated into PDMS-based microchannels and calibrated. Several combinations of sample and buffer streams with concentrations ranging from 0 to 34 mg/l DO were generated and measured for up to three independent parallel flow streams. In addition, diffusion-based stream broadening measured with the sensor was used to determine the coefficient of diffusion of O_2 in the flow medium. The devices have the potential to provide novel insights into cell biology and improve the relevance of *in-vitro* cell assays.**

***Index Terms*—Microfluidics, hydrodynamic focusing, optical oxygen sensor, PtOEPK/PS, spatial measurement.**

I. Introduction

THE characteristics of laminar flow, as observed in microfluidic devices, allow one to generate parallel multi-stream flows with stable inter-stream interfaces in a single microchannel. Material transport across these interfaces is by diffusion only and can be controlled using the flow speed of the individual streams. In cell biology, this phenomenon can be applied to produce controlled chemical microenvironments down to sub-cellular dimensions [1, 2], enabling one to study the biochemical and biophysical processes of cells. To this day the use of multiple parallel flow streams has been explored mostly for the partial treatment of individual and patterned cells with biochemical reagents [1-3]. In an extension of this concept, it has further been shown that the shape of the interface between the parallel flow streams can be selectively modified by modulating the driving pressures to produce arbitrary shaped chemical signal streams [4].

Beyond the use for the delivery of reagents or nanoparticles, multi-stream laminar flows also have the potential to be used to generate microenvironments with controlled oxygen concentrations inside a single channel. In cell-based applications in particular, the oxygen concentration of a sample stream itself represents a parameter with significant effect on cellular development and function. For example, the dissolved oxygen (DO) concentration has been found to be intimately linked to cell survival, metabolism and function [5, 6]. The capability to expose regions of a cell-culture or individual cells and regions on the cell surface to controlled DO levels therefore has the potential to yield novel insights into cell biology. Furthermore, measuring and controlling the DO concentrations of sample streams will increase the relevance of existing small-molecule delivery applications, which previously have been performed mostly with media equilibrated under atmospheric oxygen conditions [1-4, 7].

Achieving this requires a means of measuring spatially-distributed DO concentrations inside the particular microdevice. Thus, we have recently developed a robust deposition and patterning method for optical oxygen sensors based on Platinum(II) octaethylporphyrin ketone (PtOEPK) in polystyrene (PS) as microporous oxygen-permeable matrix [8]. This material system has attracted considerable interest due to the long wavelength shift and long-term photo stability exhibited by the PtOEPK molecule [9]. In addition, the homogeneous nature of spin-coated sensor films as obtained with our fabrication process allows one to visualize spatially-varying DO concentrations in-situ, such as generated by two independent flow streams [8].

In this paper we extend the concept by demonstrating the advanced capabilities of the integrated sensor system for spatially-resolved measurement of DO in two microfluidic devices related to the generation of localized microenvironments. The in-situ measurement of local oxygen concentration is demonstrated both in flow streams hydrodynamically focused to cellular dimensions, as well as multiple parallel streams with variable concentration levels. The former represents an important example of how the spatial resolution of applied stimuli, such as oxygen, can be improved towards cellular and sub-cellular dimensions. While this has previously been demonstrated as a means to improve the sample control for small molecular reagents [7], this paper

Manuscript received. This work was supported in part by the University of Canterbury through a Targeted Doctoral Scholarship and the MacDiarmid Institute for Advanced Materials and Nanotechnology through a Post Doctoral Fellowship. Part of this paper was presented in an earlier version at the 2009 IEEE SENSORS Conference and was published in its proceedings.

V. Nock is with the MacDiarmid Institute for Advanced Materials and Nanotechnology, Department for Electrical and Computer Engineering, University of Canterbury, Christchurch, Private Bag 4800, New Zealand (phone: +643364 2987 ext 7123; e-mail: volker.nock@elec.canterbury.ac.nz).

R. J. Blaikie is with the MacDiarmid Institute for Advanced Materials and Nanotechnology, Department for Electrical and Computer Engineering, University of Canterbury, Christchurch, Private Bag 4800, New Zealand (e-mail: richard.blaikie@canterbury.ac.nz).

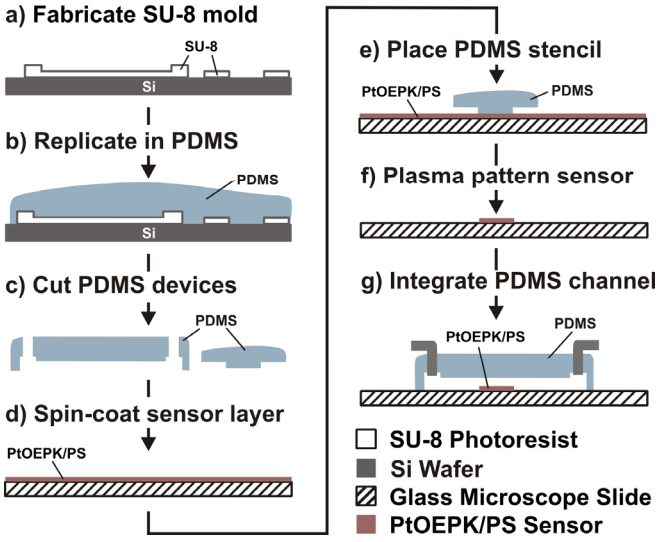

Fig. 1 Schematic of the device fabrication process.

shows for the first time how this principle can be extended to the delivery of biologically relevant oxygen.

The latter example demonstrates the use of the sensors to control oxygen in parallel molecule delivery cell-network assays for active exposure of cultures to locally different oxygen concentrations within a single device. In addition, we show how the integrated sensor can be used, similar to a T or H-filter [10, 11], to measure the coefficient of diffusion of oxygen for the perfusion media in this specific configuration.

II. Experimental

A. Device Fabrication

The sensor etch stencils and the channel devices for multi-stream laminar flow and hydrodynamic focusing were fabricated using lithography and replica-molding in poly-dimethylsiloxane (PDMS, Sylgard 184, DowCorning) [12]. Details of the fabrication process and integration of the bio-compatible oxygen sensor layer via soft-lithography have been described previously [8]. Figure 1 shows a schematic of the main fabrication steps.

In brief, micro-scale patterns were created using computer-aided design software (L-Edit, Tanner Inc) and then transferred onto chrome covered glass masks (Nanofilm) using a laser mask writer (µPG101, Heidelberg Instruments). The masks were used for photolithographic reproduction in a mask aligner (MA 6, Suss Microtec) with 4" Si wafers as substrates and negative tone photoresist (SU-8 2100, MicroChem). To create the resist molds, patterns on the mask were transferred into SU-8 through exposure and subsequent development in (1-methoxy-2-propyl)acetate (Fig. 1(a)). After rinsing with isopropanol and blow-drying with nitrogen, the molds were treated with trimethylchlorosilane (TMCS, Sigma Aldrich) to facilitate removal of the cured polymer.

Degassed PDMS pre-polymer mixture (10:1 w/w Sylgard 184, Dow Corning) was cast onto the photoresist/silicon wafer mold master and cured at 80˚C for 3 hrs on a hotplate (Fig. 1(b)). Once cured, stencils and devices were peeled off and cut to size (Fig. 1(c)). In case of the microchannel devices, inlet and outlet holes were created using a biopsy punch (Stiefel).

The oxygen sensor films were formed on glass microscope slides (Proscitech) by spin-coating a 7% w/w solution of PS (Sigma Aldrich) and PtOEPK (Frontier Scientific) in toluene to a typical thickness of 400 nm (Fig. 1(d)). After evaporation of the solvent, pre-fabricated PDMS stencils were brought into conformal contact with the sensor films (Fig. 1(e)) and a reactive ion etcher (RIE, Plasmalab 80, Oxford Instruments) was used to pattern the films in oxygen plasma (Fig. 1(f)).

After patterning, the PDMS microchannel devices were sealed to the glass substrates with the PtOEPK/PS sensors by surface activation in atmosphere using a corona wand (BD-20AC, Electro Technic Products). The final fabricated structure is shown in Fig. 1(g).

B. Fluidic Control

Figure 2 shows a schematic of the spatially-resolved oxygen measurement setup. A dual syringe pump (PHD 2000, Harvard) with syringes of different sizes was used to provide pressure-driven flow through the gas exchangers and the microchannel devices. A custom bubble-trap connected via tubing (Tygon, Cole-Parmer) to the system components and placed after the syringe pump before the gas exchangers, was used to remove any initial air bubbles from the flow. Prior to use, the sensor film response was calibrated using a flow-through Clark-electrode oxygen sensor (DO-166FT, Lazar Research) connected between the gas exchanger outlets and the microchannel inlets. Deionized (DI) water could be oxygenated in the gas exchangers from 0 mg/l (using oxygen-free nitrogen gas, BOC) up to a maximum DO concentration in water of 34 mg/l (using industrial grade oxygen gas, BOC).

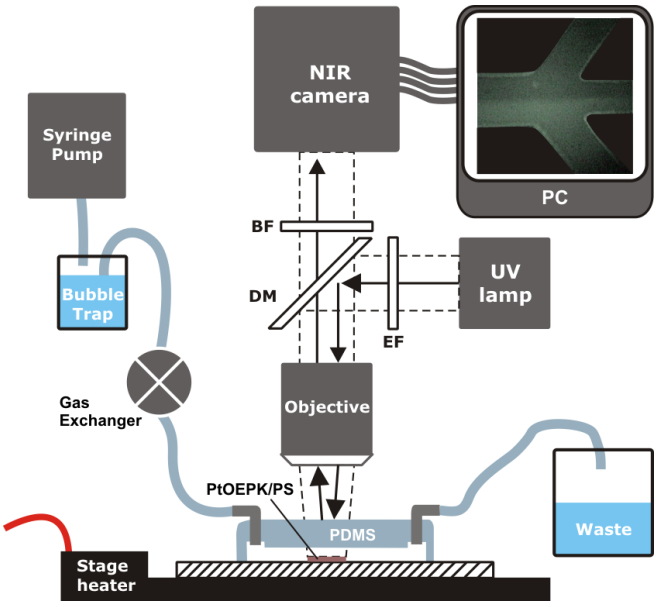

Fig. 2 Schematic of the experimental oxygen measurement setup.

C. *Oxygen Measurement*

Dissolved oxygen measurements were performed using a standard fluorescence microscope (Nikon Eclipse 80i) in combination with custom filter cube (Chroma) and a digital camera (Sony Handycam) sensitive in the near-infrared (NIR) for image acquisition. This is necessary since the PtOEPK dye exhibits an absorption peak at 590 nm (EF) and an emission peak at 760 nm (BF) in the NIR. During measurements the device was placed on a microscope stage heater (LEC Instruments) and held at a constant temperature of 37°C, corresponding to cell-culture conditions. Digital images of the recorded change of PtOEPK fluorescent dye intensity in presence of molecular oxygen were analyzed using the image processing module of Matlab (Mathworks) and a pre-recorded Stern-Volmer calibration curve, as demonstrated previously [8]. Results of the oxygen diffusion coefficient measurements were compared to computational fluidic simulations (CFD) of a 2D model using Multiphysics (V3.5a, Comsol) [13].

III. Results and Discussion

Figure 3 shows photographs of the gas exchanger and the assembled hydrodynamic focusing and multi-stream devices. To create bubble-free flow of defined oxygen concentrations two dual-layer diffusion-based gas exchangers were fabricated in PDMS using a modified version of the replica molding technique described before. The photograph on the left of Fig. 3(a) shows one of the gas exchangers filled with blue and red colored water indicating the liquid and gas layers, respectively. The thickness of the gas-permeable membrane, shown as SEM micrograph on the right in Fig. 2(a), between the liquid and gas carrying channels was controlled to around 30 µm by spin-coating PDMS pre-polymer onto the photoresist mold and subsequent curing for 10 min at 80˚C. A second pre-cured PDMS layer was then aligned onto this and both cured for further 2 hrs [14]. Using the Clark-electrode sensor the gas exchangers were measured to provide a maximum dissolved oxygen concentration of 34 mg/l in water.

Figure 3(b) shows a photograph of the hydrodynamic focusing device with tubing inserted and mounted on the microscope stage heater. Red-colored water was used to indicate the buffer inlet (flow rate V_1, initial DO concentration $c_{O2,1}$), which is divided into two channels to provide the side buffer streams for focusing. The central sample stream (flow rate V_2, initial DO concentration $c_{O2,2}$) is indicated by the blue-colored channel. Buffer and sample streams were combined in a 200 µm wide rectangular microchannel with a total length of 100 mm and a common outlet.

The multi-stream flow device is shown in Fig. 3(c) together with two external gas exchangers on separate substrates and connecting tubing. Central to the device is a rectangular parallel-plate microchannel with integrated oxygen sensor film and three inlets and a common outlet. The output flows with varying oxygen concentration from the three gas exchangers are combined in this channel to yield the parallel laminar flow streams. Blue and red-colored water were used in Fig. 3(c) to visualize the fluidic and gas layers of the device, respectively.

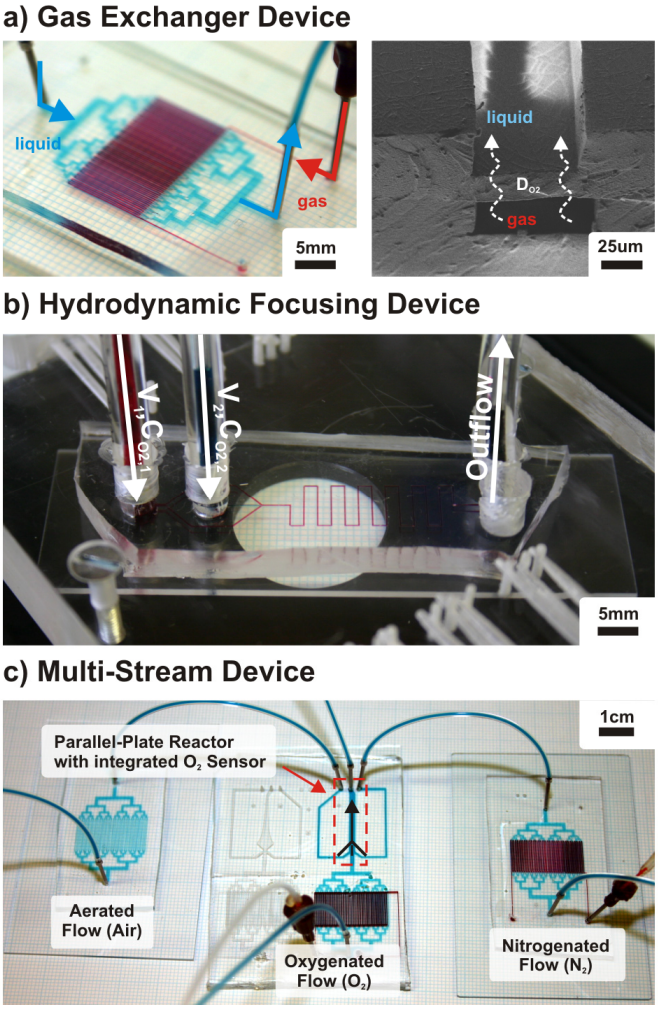

Fig. 3 Photographs of the flow devices used for the experimental demonstration of generation and detection of spatially-varying oxygen concentrations. (a) Photograph of the two-layer PDMS based gas-exchanger (left) and SEM image of the internal PDMS membrane (right) used to produce bubble-free inlet flows with controlled oxygen concentration. Red and blue colored water was used to visualize the gas and fluidic layers, respectively. (b) Photograph of the hydrodynamic focusing device mounted on the microscope heater. Two inlets supply the central sample stream (blue) and the buffer streams (red), leading to a combined outlet via a meandering microchannel with integrated oxygen sensor. (c) Photograph of the multi-stream laminar flow device with attached gas-exchangers. Inlet flows from three exchangers combine in the central parallel-plate microchannel with subjacent sensor film. Colored water indicates gas (red) and fluidic (blue) layers, respectively.

In the following the use of the two devices with integrated sensors for oxygen control and visualization is demonstrated. The syringe pump and gas exchangers were used to provide bubble-free inlet flows of DI water with different DO concentrations. These were chosen to correspond to hypoxia (0 mg/l O_2), aerated water (~8.6 mg/l O_2) and fully saturated hyperoxic water (34 mg/l O_2). Depending on the application, additional concentrations within this range can be produced by simply adjusting the gas mixture used in the gas exchangers.

Several combinations of buffer and sample stream concentrations and flow rates were used. The oxygen concentration in the devices was visualized using fluorescence microscopy on the subjacent PtOEPK/PS layer. The main advantages of this thin-film sensor system rest on the solid-state nature of the film combined with the optical sensor read-out allowing for non-contact measurements inside fully enclosed devices. Especially compared to other dissolved oxygen probes, the PtOEPK/PS sensor films are less expensive due to being reusable and, through encapsulation in the PS matrix, are less likely to influence the measurement by interacting with cells and microorganisms cultured inside the device.

A. Hydrodynamically Focused Flow

Figure 4 shows the generation and spatially-resolved detection of hydrodynamically focused flow streams with controlled oxygen concentrations [15]. With a single pump and the syringe sizes available, typical buffer/sample flow rate combinations from 0.1 to 0.5 ml/min could be produced. As indicated by the brightfield micrograph in Fig. 4(a), oxygen-dependent fluorescence intensity images were recorded at different positions along the meandering microchannel. Figures 4(b)&(c) show the intensity image of the sensor film inside the microchannel at the inlet and 64 mm downstream, respectively and as indicated by the dashed black rectangles in Fig. 4(a). For this example the oxygen concentration of the buffer streams was set to hypoxia (0 mg/l O_2) and that of the sample stream to hyperoxia (34 mg/l O_2). The outline of the microchannel in the images (dashed white lines) indicates the capability of the sensor to resolve the different DO levels inside the channel.

This configuration of the sample stream would for example, allow one to study spatially-resolved the reversible growth inhibition and differentiation exhibited by individual fibroblasts when exposed to high oxygen levels [14]. For neural and other stem cells in comparison, hypoxic conditions were observed to promote growth and influence differentiation [16]. Switching to these conditions is easily realized in the presented device by changing the gases used in the gas exchangers to yield a hypoxic sample stream (N_2) and saturated buffer streams (O_2). Figure 4(d) shows the intensity image corresponding to this particular configuration at the same location as Fig. 4(b). In both cases the oxygen concentration of the buffer streams (and sample stream) can be finely tuned to the desired experimental conditions within the full range produced by the gas exchangers.

In addition to the visualization of the DO content of the flow streams, the intensity response of the sensor film can also be used to measure the absolute concentration. This is achieved by pre-calibration of the intensity change with flows of known oxygen concentrations. The calibration curve is then used to convert the change in intensity for an unknown concentration to the corresponding oxygen value in mg/l. Due to the homogeneous films obtained with our fabrication method and by using fluorescent intensity quenching for

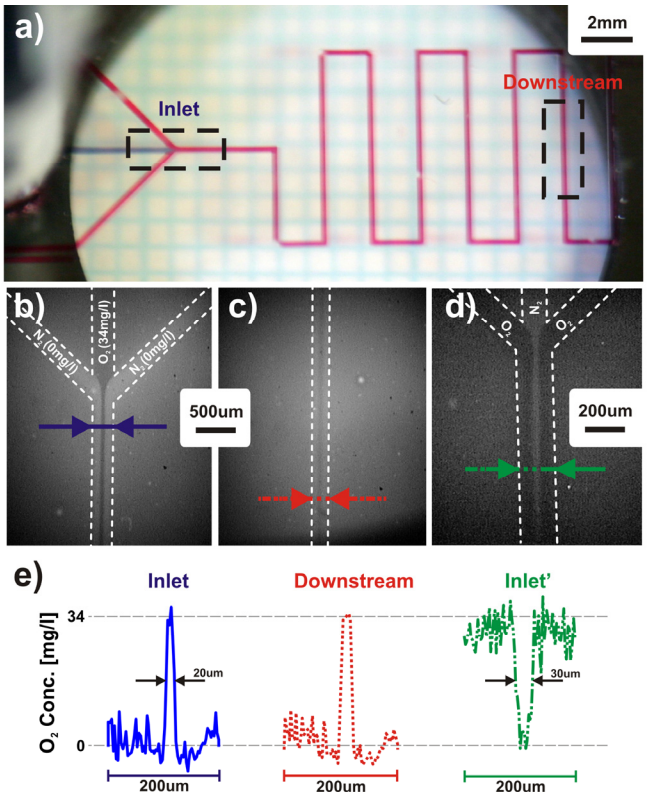

Fig. 4 Visualization of oxygen concentrations in hydrodynamically focused flow. (a) Micrograph of the microchannel showing the central sample stream (blue) and buffer streams (red). Dashed rectangles indicate the measurement locations at the inlet and ~6 cm downstream. (b)-(d) Oxygen-dependent optical intensity images of the sensor film at the measurement locations indicated in a). Regions of higher and lower intensity indicate lower and higher oxygen concentrations, respectively. In b) and c) the central sample stream corresponds to a DO concentration of 34 mg/l (hyperoxia) and the buffer streams to 0 mg/l (hypoxia), whereas in d) the concentrations are inverted to yield a hypoxic sample stream. (e) Calibrated plots of the oxygen concentration across the channel at the locations indicated by the arrows in b), c) and d). The oxygen-rich sample stream of b) and c) remains focused to a width of ~20 µm over the full length of 64 mm, while the oxygen-depleted stream from d) indicates device versatility.

detection, the sensor can thus be used for spatially-resolved oxygen sensing [8]. Figure 4(e) shows pre-calibrated plots of the DO concentration profile across the channel width close to the focus point (blue, green) and 64 mm downstream (red). As can be observed, hydrodynamic focusing can be used to produce a dimensionally well-defined stream with stable oxygen concentration over long flow lengths. Only minor broadening of the hyperoxic sample stream occurs, which is due to lateral oxygen diffusion over the extended channel length and can be controlled via the flow rate. The cross-channel plot for a hypoxic sample stream is shown on the right of Fig. 4(e) and demonstrates the range of conditions the device can generate and detect. The noise on the sensor signal is due mainly to the camera used for image acquisition and could be improved using a dedicated cooled camera.

Due to our interest in the cell biology of hepatocyte liver cells (∅ ~ 20 µm) and endometrial cancer cells (∅ ~ 35 µm), we have currently optimized the flow conditions to yield a sample stream width of around 20 µm

(see Fig 4(e)). If needed, this can be further reduced significantly by adjusting the buffer/sample stream flow ratio and by using a second syringe pump. Stable sample streams of widths as small as 50 nm have been reported for mixing applications [17]. While sample streams of these dimensions would enable the high-resolution stimulation of certain areas on the surface of a single cell, the resulting fluid shear forces would have to be closely monitored to not influence the cell physiology and thereby reduce the relevance of the delivered stimuli.

B. Multi-stream Flow

A second application for the oxygen sensor films can be found with chip-based multi-stream assays for cell-cell networks [3]. Figure 5 shows the generation and spatially-resolved visualization of parallel laminar flow streams with variable dissolved oxygen concentrations in such a device. To demonstrate device applicability the resulting flow was imaged and analyzed using the oxygen sensor film integrated on the bottom of the channel. Upon entering the central parallel-plate microchamber, shown in Fig. 5(a), the parallel streams remain separated over the total length of 18 mm due to the predominant laminar flow regime. This results in three distinct oxygen concentration levels being generated across the width of the chamber. Figure 5(b) shows the corresponding intensity images recorded via the integrated sensor film for (from left to right) the reactor inlet, mid-point and outlet. Aerated water (~8.6 mg/l) enters the chamber through the top inlet, oxygenated (34 mg/l) through the central and nitrogenated (0 mg/l) through the bottom inlet. The difference in oxygen concentration between the individual streams is easily discernible and remains stable over the full length of the device.

Oxygen concentration across the reactor was analyzed in the areas indicated by the dashed rectangles, inlet (red) and outlet (green), respectively. The two measurement points are separated along the length of the reactor by a distance of 16.4 mm. Figure 5(c) shows the cross-width plots of the DO concentration at inlet and outlet obtained from the intensity images. The oxygen concentration levels of oxygenated, aerated and nitrogenated water, indicated in the plots in Fig. 5(c) were determined through calibration of the sensor prior to measurement. As can be observed, the width of the individual streams or oxygen levels varies over the reactor length. These differences in level width from inlet to outlet of the individual streams can partially be attributed to lateral diffusion of oxygen from the oxygen-rich central stream. However, in addition to the diffusion contribution, the flow rate of the nitrogenated stream (bottom in intensity images, right in concentration plot) was found to be slightly less than the inlet flow rate of 0.1 ml/min pre-set via the syringe pump. The difference originated in the uneven number of inlets, where one of the two syringes on the pump was used to supply two inlets each via a y-junction in the tubing. Although the second half of flow from the syringe, providing the nitrogenated stream, was connected to an additional dummy

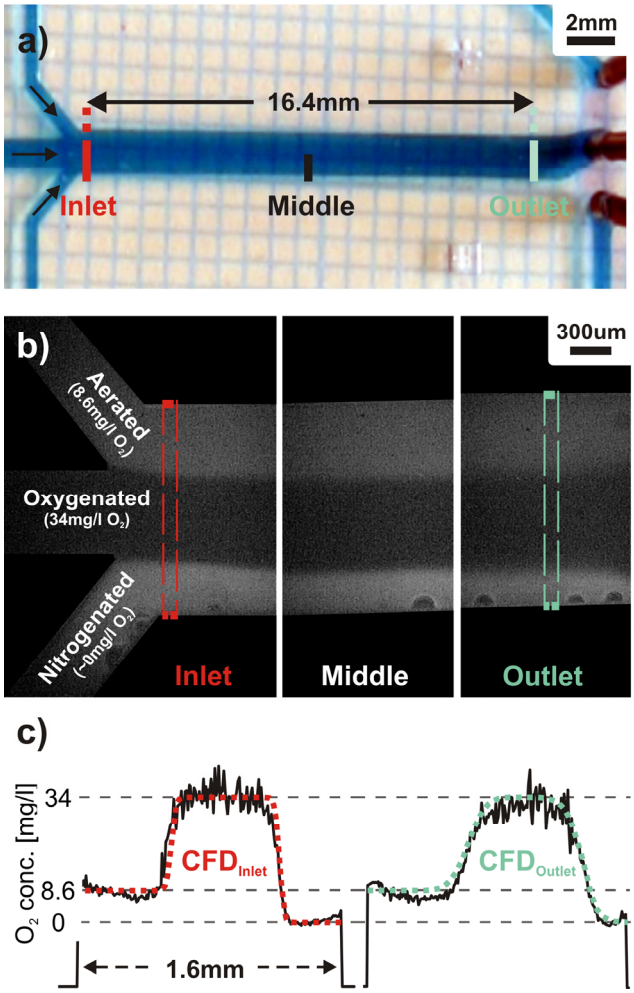

Fig. 5 Visualization and measurement of oxygen in multi-stream laminar flow. (a) Micrograph of the parallel-plate rectangular microchannel with integrated optical oxygen sensor film indicating device dimensions, measurement locations and flow layout. (b)Oxygen-dependent fluorescent intensity images recorded at the inlet, middle and outlet. The intensity response for the top stream corresponds to aerated (8.6 mg/l O_2), the middle stream to hyperoxic (34 mg/l O_2) and the bottom stream to hypoxic (0 mg/l O_2) conditions. Inter-stream boundaries remain stable over the full channel length of 18 mm. (c) Oxygen concentration plots across the channel width at positions indicated by the dashed rectangles in (b). Concentration levels (dashed lines) were obtained through calibration of the sensor prior to use and coincide well with the individual streams. By applying diffusion theory, a coefficient of diffusion of oxygen in water of $D_{O2} = 2.57 \times 10^{-5}$ $cm^2 s^{-1}$ can be calculated from the decrease in slope from the inlet to outlet profile. This compares well with CFD simulation results obtained using the measured coefficient as parameter and overlaid as dotted lines in the plot.

gas-exchanger for fluidic resistance equilibration, combining only one of these two streams in the reactor lead to the aforementioned differences in stream width. If perceived critical, this minor problem could be mitigated by use of a triple syringe pump with one single syringe per stream or by a device design with only even number of inlets.

The more important observation from Fig. 5(c) however, is the significant decrease in slope of the transition between the centre stream and the two outlaying ones from inlet to the outlet plot. This is indicative of lateral diffusion of oxygen from the central oxygenated stream to regions of lower oxygen concentration (aerated and nitrogenated streams).

Since the device dimensions, initial oxygen concentrations of the three streams and the flow conditions are known, this phenomenon can be used to deduce the diffusion coefficient of oxygen in the fluid using Fick's Law [13]. By solving the diffusion equation the coefficient of diffusion is found as a function of the characteristic length

$$D_{O2} = \frac{x^2}{4 \cdot t}, \quad (1)$$

where D_{O2} is the coefficient of diffusion of oxygen in the medium, t the residence time in the channel and x is the diffusion length perpendicular to the flow direction. For a total flow rate of 0.3 ml/min the residence time t = 1.05 s and the diffusion length x can be deduced from the difference of the slopes in the inlet and outlet plots in Fig. 5(c) to x = 104 µm in our case. Thus, using the oxygen sensors the coefficient of diffusion for oxygen in water at a temperature of 37°C was determined to be $D_{O2} = 2.57 \times 10^{-5}$ $cm^2 s^{-1}$. This value compares well with oxygen diffusion coefficients in water of 2.52×10^{-5} $cm^2 s^{-1}$ at 35.1ºC and 2.78×10^{-5} $cm^2 s^{-1}$ at 40.1ºC published in literature [18].

To further validate this result, the measured oxygen distribution was compared to a 2D CFD simulation of the microchannel using the experimental geometry, the flow conditions and the measured coefficient of diffusion as model parameters [13]. Flow conditions were modeled using the Navier-Stokes application mode with three parallel inlet streams of equal flow rate Q = 0.1 ml/min each. The pressure at the outlet was set to p = 0. Liquid properties used were those of freshwater with a dynamic viscosity $\eta = 1 \times 10^{-3}$ Pa*s and density $\rho = 1 \times 10^3$ kg/m^3. Species transport was modeled using the Convection and Diffusion application mode. The measured D_{O2} of 2.57×10^{-9} $m^2 s^{-1}$ was used as the isotropic diffusion coefficient of the liquid. Each inlet was assigned a constant species concentration of 0, 0.538 and 2.125 mol/m^3, respectively. The boundary condition of the outlet was set to convective flux and the two application modes were coupled via the fluid velocity u, parallel to the long axis of the reactor chamber. Automated meshing and refinement yielded a 90.000 element mesh, which was solved using the GMRES linear system solver.

Simulated oxygen concentration profiles across the chamber width were evaluated at the two points indicated in Fig. 5(a). The simulation results are plotted as dotted lines superimposed onto the measured profiles in Fig. 5(c). As can be seen, good agreement exists between the shape of the measured and the simulated concentration profiles at both the inlet and outlet and considering the noise on the measured data. In addition, the slope of the profiles coincide, indicating the validity of the diffusion model for analysis, as well as the value of the diffusion coefficient measured using the integrated optical sensor film.

In the future, cell-culture and cell micro-patterning will be integrated into the devices. As we have demonstrated recently in a similar laminar flow device, the sensor layer retains its function with extracellular matrix proteins deposited directly onto the sensor film and a layer of endometrial cancer cells cultured on top [19]. This will enable the study of the effects of oxygen concentration on cell development and function in general. It will further allow one to provide better environmental control for molecular delivery experiments, in particular by adding the ability to visualize and control the oxygen concentration of the perfusion media used to deliver the respective chemical stimuli. Similarly, and as demonstrated here, the integrated sensors have the potential to allow for the on-chip integration of inline coefficient of diffusion calibration for oxygen in the respective media prior to a cell-culture bioreactor.

IV. Conclusions

In this paper we have shown the application of an integrated optical oxygen sensor to microfluidic devices capable of generating microenvironments with controlled oxygen concentrations. Spatially-resolved in-situ measurements of DO were demonstrated for parallel laminar and hydrodynamically-focused streams and for concentrations ranging from 0 to 34 mg/l DO using the low-cost, reusable oxygen sensor film. Water-based sample streams were focused to widths of 20 µm and could be maintained over lengths exceeding 6 cm. The visualization of DO in multi-stream laminar flow was demonstrated and the device used to successfully measure the coefficient of diffusion of oxygen in water $D_{O2} = 2.57 \times 10^{-5}$ $cm^2 s^{-1}$. The presented devices provide novel tools for lab-on-a-chip based oxygen concentration dependent biological assays and cell biology experiments.

Acknowledgment

The authors would like to thank Helen Devereux and Gary Turner for technical assistance.

References

[1] S. Takayama, E. Ostuni, P. LeDuc, K. Naruse, D. E. Ingber, and G. M. Whitesides, "Laminar flows: Subcellular positioning of small molecules," Nature, vol. 411, pp. 1016-1016, 2001.

[2] S. Takayama, E. Ostuni, P. LeDuc, K. Naruse, D. E. Ingber, and G. M. Whitesides, "Selective Chemical Treatment of Cellular Microdomains Using Multiple Laminar Streams," Chem. Biol., vol. 10, pp. 123-130, 2003.

[3] H. Kaji, M. Nishizawa, and T. Matsue, "Localized chemical stimulation to micropatterned cells using multiple laminar fluid flows," Lab Chip, vol. 3, pp. 208-211, 2003.

[4] B. Kuczenski, W. C. Ruder, W. C. Messner, and P. R. LeDuc, "Probing Cellular Dynamics with a Chemical Signal Generator," PLoS ONE, vol. 4, p. e4847, 2009.

[5] S. Roy, S. Khanna, A. A. Bickerstaff, S. V. Subramanian, M. Atalay, M. Bierl, S. Pendyala, D. Levy, N. Sharma, M. Venojarvi, A. Strauch, C. G. Orosz, and C. K. Sen, "Oxygen Sensing by Primary Cardiac Fibroblasts: A Key Role of p21Waf1/Cip1/Sdi1," Circ Res, vol. 92, pp. 264-271, 2003.

[6] H. Zhang and G. Semenza, "The expanding universe of hypoxia," J. Mol. Med., vol. 86, pp. 739-746, 2008.

[7] Fen Wang, Hao Wang, Jun Wang, Hsiang-Yu Wang, Peter L. Rummel, Suresh V. Garimella, and Chang Lu, "Microfluidic delivery of small molecules into mammalian cells based on hydrodynamic focusing," Biotechnol. Bioeng., vol. 100, pp. 150-158, 2008.

[8] V. Nock, R. J. Blaikie, and T. David, "Patterning, integration and characterisation of polymer optical oxygen sensors for microfluidic devices," Lab Chip, vol. 8, pp. 1300-1307, 2008.
[9] D. B. Papkovsky, G. V. Ponomarev, W. Trettnak, and P. O'Leary, "Phosphorescent Complexes of Porphyrin Ketones: Optical Properties and Application to Oxygen Sensing," Anal. Chem., vol. 67, pp. 4112-4117, 1995.
[10] M. S. Munson, K. R. Hawkins, M. S. Hasenbank, and P. Yager, "Diffusion based analysis in a sheath flow microchannel: the sheath flow T-sensor," Lab Chip, vol. 5, pp. 856-862, 2005.
[11] A. E. Kamholz, E. A. Schilling, and P. Yager, "Optical Measurement of Transverse Molecular Diffusion in a Microchannel," Biophys. J., vol. 80, pp. 1967-1972, 2001.
[12] D. C. Duffy, J. C. McDonald, O. J. A. Schueller, and G. M. Whitesides, "Rapid Prototyping of Microfluidic Systems in Poly(dimethylsiloxane)," Anal. Chem., vol. 70, pp. 4974-4984, 1998.
[13] V. Nock, "Control and measurement of oxygen in microfluidic bioreactors," Ph.D. dissertation, Dep. of Elect. Comp. Eng., U. of Canterbury, Christchurch, New Zealand, 2009.
[14] V. Nock, R. J. Blaikie, and T. David, "Generation and Detection of Laminar Flow with Laterally-Varying Oxygen Concentration Levels," in Proc. uTAS, San Diego, USA, 2008, pp. 299-301.
[15] V. Nock and R. J. Blaikie, "Visualization and Measurement of Dissolved Oxygen Concentrations in Hydrodynamic Flow Focusing," in Proc. 8th Annual IEEE Conference on Sensors, Christchurch, New Zealand, 2009, pp. 1248-1251.
[16] L.-L. Zhu, L.-Y. Wu, D. Yew, and M. Fan, "Effects of hypoxia on the proliferation and differentiation of NSCs," Mol. Neurobiol., vol. 31, pp. 231-242, 2005.
[17] J. B. Knight, A. Vishwanath, J. P. Brody, and R. H. Austin, "Hydrodynamic Focusing on a Silicon Chip: Mixing Nanoliters in Microseconds," Phys. Rev. Let., vol. 80, p. 3863, 1998.
[18] P. Han and D. M. Bartels, "Temperature Dependence of Oxygen Diffusion in H2O and D2O," J. Phys. Chem., vol. 100, pp. 5597-5602, 1996.
[19] V. Nock, R. J. Blaikie, and T. David, "Oxygen Control for Bioreactors and In-vitro Cell Assays," AIP Proc., vol. 1151, pp. 67-70, 2009.

Volker Nock (S'06-M'09) received the Dipl.-Ing. degree in microsystem technology from the University of Freiburg, Germany in 2005 and the Ph.D. degree in electrical and computer engineering from the University of Canterbury, Christchurch, New Zealand in 2009. His Ph.D. dissertation focused on the control and measurement of oxygen in microfluidic bioreactors.

He is currently working as a Post Doctoral Fellow with the *MacDiarmid Institute for Advanced Materials and Nanotechnology* at the University of Canterbury.

His research interests include microfluidics, bioimprinting of cells, surface patterning, optical oxygen sensors, polymer force sensors and their integration into biomedical microsystems. Dr. Nock is a member of the Association of German Engineers (VDI), the Society of Photo-Optical Instrumentation Engineers (SPIE) and the Royal Society of New Zealand (RSNZ).

Richard J. Blaikie received the B.Sc. (Hons) degree from the University of Otago, New Zealand, in 1988 and the Ph.D. degree in physics from the University of Cambridge, U.K., in 1992. For one year, he was a visiting scientist at the Hitachi Cambridge Laboratory, investigating single-electron transport effects in semiconductor nanostructures. He returned to New Zealand in 1993, taking up a position in the Department of Electrical and Computer Engineering at the University of Canterbury, where he continues as a Professor.

Blaikie is currently the Director of the *MacDiarmid Institute for Advanced Materials and Nanotechnology*, a multi-institutional New Zealand Centre of Research Excellence (www.macdiarmid.ac.nz). In 2005 was appointed by the Minister of Research, Science and Technology to serve on the *Marsden Fund Council*, which administers New Zealand's investigator-initiated research fund, and he served as the chair of the Physical Sciences and Engineering panel until early 2008.

His principal research interests are the development of low cost nanolithography techniques using near field illumination, and the utilisation of sub-wavelength-structures at sub-mm and visible wavelengths. This applied electromagnetics research led to the award of the 2001 T.K. Sidey Medal of the Royal Society of New Zealand, and in 2005 he and colleague David Melville were the first to report experimental observation of the *superlensing* at optical wavelengths using thin silver films. His research interests also include polarisation modulation in optical communications systems, modelling of semiconductor device structures, and the application of nanofabrication techniques to new electronic, optical, chemical and biological devices.